

Light Nuclei Production in Au+Au Collisions at $\sqrt{s_{NN}} = 3$ GeV within Thermodynamical Approach: Bulk Properties and Collective Flow

M. Kozhevnikova^{1,*} and Yu. B. Ivanov^{2,3,†}

¹*Veksler and Baldin Laboratory of High Energy Physics, JINR Dubna, 141980 Dubna, Russia*

²*Bogoliubov Laboratory of Theoretical Physics, JINR Dubna, 141980 Dubna, Russia*

³*National Research Center "Kurchatov Institute", 123182 Moscow, Russia*

We present results of simulations of light-nuclei production in Au+Au collisions at collision energy of $\sqrt{s_{NN}} = 3$ GeV within updated Three-fluid Hydrodynamics-based Event Simulator Extended by UrQMD (Ultra-relativistic Quantum Molecular Dynamics) final State interactions (THESEUS). The results are compared with recent STAR data. The light-nuclei production is treated within the thermodynamical approach on equal basis with hadrons. The only additional parameter related to the light nuclei is the energy density of late freeze-out that imitates afterburner stage of the collision because the light nuclei do not participate in the UrQMD evolution. It is found that the late freeze-out is preferable for deuterons, tritons, and ^3He . Remarkably, the ^4He observables are better reproduced with the standard freeze-out. This suggests that the ^4He nuclei better survive in the afterburner stage because they are more spatially compact and tightly bound objects. This is an argument in favor of dynamical treatment of light nuclei. The simulations indicate that the collision dynamics is determined by the hadronic phase. The calculated results reveal not perfect but a good reproduction of the data on bulk observables and directed flow. The elliptic flow turns out to be more intricate.

PACS numbers: 25.75.-q, 25.75.Nq, 24.10.Nz

Keywords: relativistic heavy-ion collisions, hydrodynamics, light nuclei

I. INTRODUCTION

During recent years the light-nuclei production has become again one of the central topics in studies of relativistic heavy-ion collisions. As predicted, an enhanced production of light nuclei is a promising signal of the critical endpoint (CEP) [1–3]. This prediction is based on enhancement of the nucleon attraction near the CEP due to a rapid increase of correlation length [4] and slowing down the equilibration of the density fluctuations [5] in the critical region. Abundant production of light nuclei also results from formation of baryon clusters due to spinodal decomposition associated with mechanically unstable region in the first-order phase transition [6–11]. These expectations revived interest to study of the light-nuclei production at high collision energies. At lower energies, a noticeable part of the baryon charge is emitted in the form of light nuclei. Therefore, even the proton data cannot be described without proper reproduction of the light-nuclei yield. There are different approaches to the light-nuclei production, which are still actively debated [12–15].

Coalescence is the most popular approach, see, e.g., [16–26], which however needs additional parameters for description of the light-nuclei yield. The recently developed transport models [27–34] treat light nuclei microscopically on equal basis with other hadrons. However, these transport models also require an extensive addi-

tional input for the light-nuclei description.

The thermodynamical approach does not need any additional parameters for the light-nuclei treatment. It describes the light nuclei on equal basis with hadrons, i.e. in terms of temperatures and chemical potentials. This approach was first realized within the statistical model, which fairly well described deuteron midrapidity yields [35, 36] at the energies from 7.7 to 200 GeV [37, 38] while overestimated the tritium yield by roughly a factor of two [38, 39]. The statistical model gave a good description of even hypernuclei and antinuclei [40].

Inspired by relative success of the statistical model [37–40], we implemented the thermodynamic approach to the light-nuclei production into the updated THESEUS event generator [41]. In general, this approach involves no additional parameters inherent in light nuclei, which makes its predictive power the same for light nuclei and hadrons. However, because of the lack of the (post-hydrodynamical) afterburner stage for the light nuclei we had to introduce a parameter of the late freeze-out for them [42]. This late freeze-out imitates the afterburner evolution. In Ref. [42] we considered Pb+Pb and Au+Au collisions in the collision energy range of $\sqrt{s_{NN}} = 6.4\text{--}19.6$ GeV. The updated THESEUS resulted in an imperfect but reasonable reproduction of data on bulk observables of the light nuclei, especially their functional dependence on the collision energy and light-nucleus mass.

Data on light-nuclei production in Au+Au collisions at $\sqrt{s_{NN}} = 3$ GeV were recently published [43, 44]. Apart from several Blast-Wave fits, these data on bulk properties of light nuclei were analyzed in coalescence-based 3D simulations within JAM (Jet AA microscopic trans-

*e-mail: kozhevnikova@jinr.ru

†e-mail: yivanov@theor.jinr.ru

port Model [45, 46]), SMASH (Simulating Many Accelerated Strongly-interacting Hadrons [47]), and UrQMD [48], which were presented in the STAR paper [43], as well as in the JAM-based calculation [49]. Simulations were also performed within the PHQMD (Parton-Hadron-Quantum-Molecular-Dynamics) approach [31], in which the cluster formation occurs dynamically due to interactions, and the hybrid dynamical-statistical approach [50]. These models reproduce, albeit to varying degrees, experimental trends of the data. The data on the collective flow of light nuclei at 3 GeV [44] were analyzed within the coalescence-based JAM generator, presented in Ref. [44]. These JAM simulations well describe the data.

In the present paper, the treatment of our previous paper [42] is extended to Au+Au collisions at $\sqrt{s_{NN}} = 3$ GeV. We calculate bulk properties, directed and elliptic flows of protons and light nuclei (d , t , ${}^3\text{He}$ and ${}^4\text{He}$) within the updated THESEUS approach [41] based on thermodynamic treatment of light nuclei. In contrast to the collision energy range considered in Ref. [42], the yield of the light nuclei at 3 GeV plays noticeable role in the total balance of the baryon charge.

II. UPDATED THESEUS

The THESEUS event generator [51, 52] is based on the model of the three-fluid dynamics (3FD) [18, 53] complemented by the UrQMD [48] for the afterburner stage. The 3FD takes into account counterstreaming of the leading baryon-rich matter at the early stage of nuclear collisions. This nonequilibrium stage is modeled by means of two counterstreaming baryon-rich fluids. Newly produced particles, which dominantly populate the midrapidity region, are assigned to a so-called fireball fluid. These fluids are governed by set of hydrodynamic equations coupled by friction terms, which describe the energy-momentum exchange between the fluids.

The output of the 3FD model, i.e. the freeze-out hypersurface, is recorded in terms of local flow velocities and thermodynamic quantities. The THESEUS generator transforms the 3FD output into a set of observed particles, i.e. performs the particlization. After the particlization the afterburner stage is described by the UrQMD. First applications of the THESEUS generator to description of heavy-ion collisions were demonstrated in Refs. [51, 52].

In the initial version of the THESEUS [51, 52], spectra of the so-called primordial nucleons, i.e. both observable nucleons and those bound in the light nuclei, were calculated. These spectra were intended for the subsequent use in the coalescence model [18, 54] for the light-nuclei production. Therefore, the nucleons bound in the light nuclei should be subtracted from the primordial ones in order to obtain the observable nucleons. Such subtraction is performed in the 3FD, where production of the light nuclei is calculated within the coalescence approach

[18, 54]. The initial version of the THESEUS took temperature and chemical potential fields for hadron sampling from the hydrodynamic output of the 3FD (where the clusters are not included in the EoS), and produced both hadrons and clusters within the thermodynamical approach. This led to an overestimation of the total baryon charge in the final state containing both baryons and clusters. Therefore, a compensating correction was required. Such correction was made in the updated version of THESEUS [41] by means of the recalculation of the baryon chemical potentials, proceeding from the local baryon number conservation in the system of hadrons extended by the light-nuclei species listed in Tab. I. The list of the light nuclei includes the stable nuclei [deuterons (d), tritons (t), helium isotopes ${}^3\text{He}$ and ${}^4\text{He}$], and low-lying ${}^4\text{He}$ resonances decaying into stable species [1]. The corresponding anti-nuclei are also included.

Nucleus(E [MeV])	J	decay modes, in %
d	1	Stable
t	1/2	Stable
${}^3\text{He}$	1/2	Stable
${}^4\text{He}$	0	Stable
${}^4\text{He}(20.21)$	0	$p = 100$
${}^4\text{He}(21.01)$	0	$n = 24, p = 76$
${}^4\text{He}(21.84)$	2	$n = 37, p = 63$
${}^4\text{He}(23.33)$	2	$n = 47, p = 53$
${}^4\text{He}(23.64)$	1	$n = 45, p = 55$
${}^4\text{He}(24.25)$	1	$n = 47, p = 50, d = 3$
${}^4\text{He}(25.28)$	0	$n = 48, p = 52$
${}^4\text{He}(25.95)$	1	$n = 48, p = 52$
${}^4\text{He}(27.42)$	2	$n = 3, p = 3, d = 94$
${}^4\text{He}(28.31)$	1	$n = 47, p = 48, d = 5$
${}^4\text{He}(28.37)$	1	$n = 2, p = 2, d = 96$
${}^4\text{He}(28.39)$	2	$n = 0.2, p = 0.2, d = 99.6$
${}^4\text{He}(28.64)$	0	$d = 100$
${}^4\text{He}(28.67)$	2	$d = 100$
${}^4\text{He}(29.89)$	2	$n = 0.4, p = 0.4, d = 99.2$

TABLE I: Stable light nuclei and low-lying resonances of the ${}^4\text{He}$ system (from BNL properties of nuclides [55]). J denotes the total angular momentum. The last column represents branching ratios of the decay channels, in per cents. The p, n, d correspond to the emission of protons, neutrons, or deuterons, respectively.

In the updated version of the THESEUS [41], the light nuclei were included on equal basis with other hadrons. These nuclei are sampled similarly to other hadrons, i.e. accordingly to their phase-space distribution functions. However, there is an important difference. While the hadrons pass through the UrQMD afterburner stage after the particlization, the light nuclei do not, because the UrQMD is not able to treat them. This is a definite shortcoming because the light nuclei are destroyed and

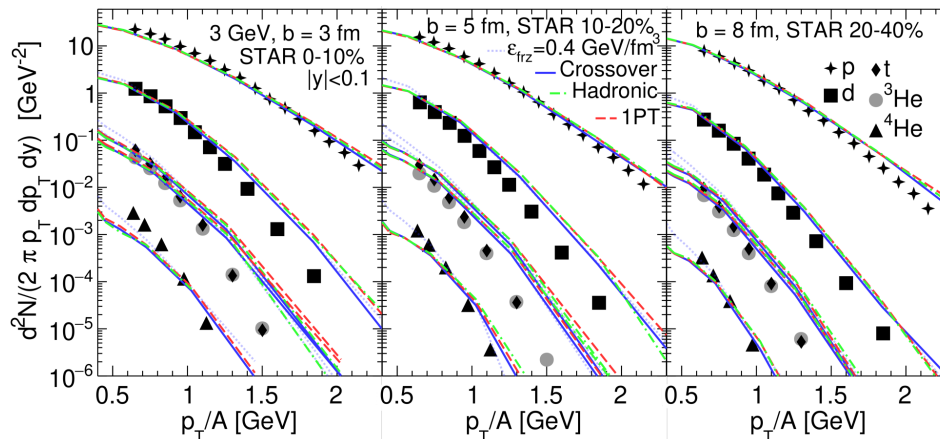


FIG. 1: Midrapidity ($|y| < 0.1$) transverse-momentum spectra of protons and light nuclei (deuterons, tritons, ${}^3\text{He}$ and ${}^4\text{He}$) in Au+Au collisions at collision energy of $\sqrt{s_{NN}} = 3$ GeV and different centralities (impact parameters b). Results are calculated with hadronic, 1PT and crossover EoS's. Results of the THESEUS simulations with the late freeze-out ($\varepsilon_{\text{frz}} = 0.2$ GeV/fm 3) for three EoS's and the conventional 3FD freeze-out ($\varepsilon_{\text{frz}} = 0.4$ GeV/fm 3) for the crossover EoS are displayed for light nuclei. Protons are calculated within the conventional 3FD freeze-out with the subsequent UrQMD afterburner. STAR data are from Ref. [43].

again re-produced during the afterburner stage [27, 28, 30, 32, 33]. Following the recipe of Ref. [41], we imitate the afterburner for light nuclei by late freeze-out in the 3FD.

Three different equations of state (EoS's) are used in the 3FD simulations: a purely hadronic EoS [56] (had. EoS) and two EoS's with deconfinement [57], i.e. an EoS with a first-order phase transition (1PT EoS) and one with a smooth crossover transition (crossover EoS). Consequently, the 3FD output for these EoS's is used in the THESEUS generator.

III. BULK OBSERVABLES

To partially overcome the aforementioned problem of the afterburner stage for the light nuclei, we imitate the afterburner effect by late freeze-out for light nuclei. Similarly to Ref. [41], we take the freeze-out energy density $\varepsilon_{\text{frz}} = 0.2$ GeV/fm 3 for this late freeze-out, which looks quite suitable for all considered quantities, as seen below. No other additional tuning of the parameters was carried out for the light nuclei. Note that the conventional 3FD freeze-out energy density for all other hadrons, subjected to the UrQMD afterburner, is 0.4 GeV/fm 3 . Details of the freeze-out procedure in the 3FD are described in Refs. [58, 59]. The ε_{frz} quantity has meaning of a “trigger” that indicates possibility of the freeze-out. The freeze-out procedure begins when the local (i.e. in a cell) energy density drops below the freeze-out value ε_{frz} , then testing for additional freeze-out conditions starts. If all the freeze-out conditions are met, the cell is declared frozen-out. Thus, the actual energy density of a frozen-out cell turns out to be lower than ε_{frz} , as it is demonstrated, e.g., in Ref. [60].

A. Transverse-momentum spectra

Midrapidity ($|y| < 0.1$) transverse-momentum spectra of protons and light nuclei (deuterons, tritons, ${}^3\text{He}$ and ${}^4\text{He}$) in Au+Au collisions at collision energy of $\sqrt{s_{NN}} = 3$ GeV and different centralities (impact parameters b) are displayed in Fig. 1. The proton spectra are calculated within full THESEUS, i.e. with the standard 3FD freeze-out and the UrQMD afterburner. The spectra of light nuclei are evaluated for the late 3FD freeze-out without the afterburner stage. As seen, the results for different EoS's are almost identical, which means that the dynamics is dominated by the hadronic phase. The difference between the late freeze-out and the conventional 3FD freeze-out for the crossover EoS is mostly seen at low p_T for light nuclei. In the p_T spectra, this difference does not look dramatic. However, in rapidity distributions, Fig. 2, which mostly determined by the low- p_T spectra, the difference is quite noticeable.

Similarly to that found previously [42], the experimental p_T spectra [43] turn out to be steeper than the calculated ones. This is not only the problem of light-nuclei description. The proton spectra are also more flat than the experimental ones. This is a shortcoming of the 3FD model. The slight extra flatness of the proton spectra transforms into larger extra flatness of light-nuclei spectra.

As has been already noted in Ref. [42], the 3FD predictions overestimate the high- p_T ends of the spectra because of finiteness of the considered system. Even abundant hadronic probes become rare at high momenta. For the rare probes, treatment on the basis of the canonical ensemble is needed rather than within the grand canonical ensemble. The grand canonical ensemble results in overestimation of their yields. Of course, it is difficult to

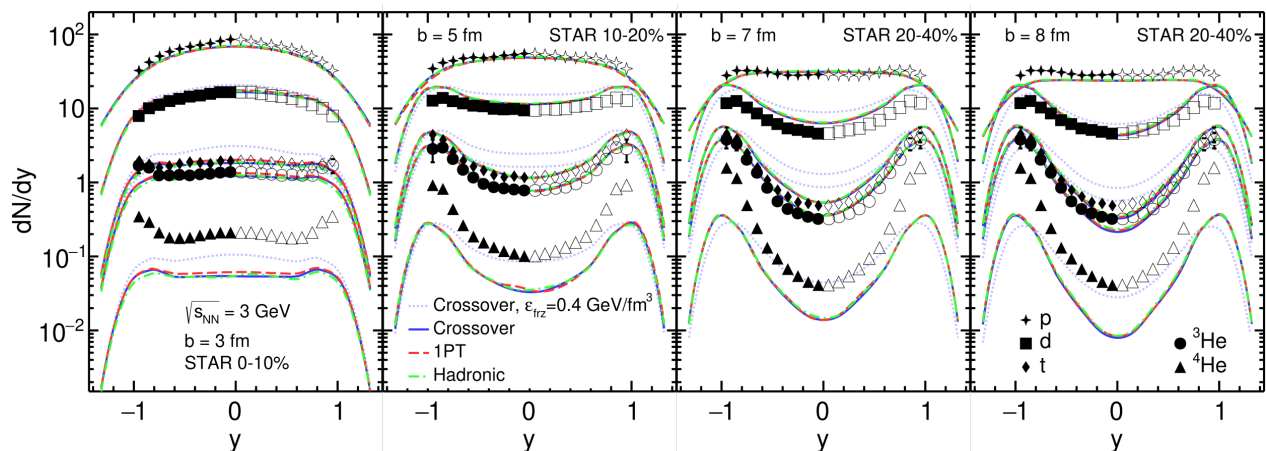


FIG. 2: Rapidity distributions of protons and light nuclei (deuterons, tritons, ${}^3\text{He}$ and ${}^4\text{He}$) in Au+Au collisions at collision energy of $\sqrt{s_{NN}} = 3$ GeV and different centralities (impact parameters b). Results are calculated with hadronic, 1PT and crossover EoS's. Results of the THESEUS simulations with the late freeze-out ($\varepsilon_{\text{frz}} = 0.2$ GeV/fm 3) for three EoS's and the conventional 3FD freeze-out ($\varepsilon_{\text{frz}} = 0.4$ GeV/fm 3) for the crossover EoS are displayed for light nuclei. Protons are calculated within the conventional 3FD freeze-out with the subsequent UrQMD afterburner. STAR data are from Ref. [43]. Full symbols display measured experimental points, whereas the open ones are those reflected with respect to the midrapidity.

indicate how much of this overestimation is due to the grand canonical treatment, and not to the shortcomings of the model.

B. Rapidity distributions

Rapidity distributions of protons and light nuclei in Au+Au collisions at collision energy of $\sqrt{s_{NN}} = 3$ GeV and different centralities are presented in Fig. 2. Again the proton distributions are calculated within full THESEUS, i.e. with the standard 3FD freeze-out and the UrQMD afterburner, while the light-nuclei distributions, within the late 3FD freeze-out and without the afterburner stage. The light-nuclei distributions, calculated at the conventional 3FD freeze-out, are also displayed for comparison. The same value of the late-freeze-out energy density ($\varepsilon_{\text{frz}} = 0.2$ GeV/fm 3) as that at higher collision energies [42] turned out to be the most suitable at 3 GeV. The reproduction of the experimental distributions turns out to be even better than that at higher collision energies [42]. The THESEUS simulations well describe difference in the form of proton and light-nuclei distributions and its dependence on the centrality.

For the experimental centrality of 20-40% we present comparison with results for two impact parameters ($b = 7$ and 8 fm) in order to illustrate the sensitivity of the results to the choice of b . As seen, the proton rapidity density is underestimated in midrapidity at $b = 8$ fm in spite of perfect reproduction of the low- p_T experimental spectrum, see Fig. 1. The reason is that the extrapolation of the experimental spectrum to even lower p_T exceeds the THESEUS predictions. Similar situation takes place for the light nuclei. Thus, the results for two impact parameters ($b = 7$ and 8 fm) illustrate uncertainty

of the THESEUS predictions.

The ${}^4\text{He}$ distributions deserve a separate discussion. The late-freeze-out calculation strongly underestimates these distributions. Expanding the list of light-nuclei resonances by those of ${}^5\text{H}$, ${}^5\text{He}$, and ${}^5\text{Li}$ [38], which decay into ${}^4\text{He}$, makes an additional contribution to the ${}^4\text{He}$ yield. This additional contribution is large, i.e. of the order of 60%, in central collisions at the energy of 3 GeV, accordingly to Ref. [38]. However, it is not large enough to compensate the obtained underestimation. At the same time, the standard-freeze-out calculation results in much better (almost perfect in midrapidity at 10-20% and 20-40% centralities) reproduction of the data. The p_T spectra are also much better described by the standard freeze-out, see Fig. 1. This suggests that the ${}^4\text{He}$ nuclei better survive in the afterburner stage because they are more spatially compact and tightly bound objects. Then the standard freeze-out is more relevant for their description. Note that the feed-down contribution to the ${}^4\text{He}$ yield, $\approx 60\%$ [38], is quite enough to drastically improve the reproduction midrapidity data in central collisions by the standard-freeze-out calculation.

At lower collision energies, the enhancement of the ${}^4\text{He}$ production is even more spectacular [61]. In central Au+Au collisions, the ${}^4\text{He}$ and ${}^3\text{He}$ yields are approximately equal at $E_{\text{lab}} = 0.4A$ GeV and the ${}^4\text{He}$ yield even exceeds that of ${}^3\text{He}$ at $0.15A$ GeV. It seemingly contradicts to the thermodynamic picture of the light-nuclei production. However, this contradiction is removed, if the chemical freeze-out occurs earlier for ${}^4\text{He}$ nuclei than for d , t and ${}^3\text{He}$ because of larger binding energy of the ${}^4\text{He}$ nuclei. In Ref. [34] it is formulated in terms of the Mott transition [62]: The observed enhancement of the ${}^4\text{He}$ yield can be attributed to the weaker Mott effect on ${}^4\text{He}$ nuclei than that on deuteron, triton and ${}^3\text{He}$, as a

result of its much larger binding energy. The cutoff value for the average nucleon phase-space density, f_A^{cut} , that is used in Ref. [34], see Eq. (5) in Ref. [34], in fact plays the role of the effective freeze-out for different light nuclei. As found in Ref. [34], the $f_{A=4}^{\text{cut}}$ value is approximately twice as large as that for lighter nuclei. This is consistent with our conclusion about the earlier freeze-out of ${}^4\text{He}$. In particular, the results of the kinetic approach of Ref. [34] imply that the freeze-out parameters for each light-nuclei specie are individual and depend on the binding energy of considered nucleus.

C. Medium Effects

Study of the in-medium effects in light-nuclei production has started long ago [63]. Later, coupled quantum kinetic equations were derived which describe the time evolution of the Wigner distribution functions for nucleons and light clusters [64]. An alternative approach has also been proposed within the antisymmetrized molecular dynamics (AMD) approach [65], in which nucleons are represented in terms of quantal wave packets, which are antisymmetrized with each other. These approaches have been successfully applied to analysis of results of the GANIL experiment at 50A MeV.

In Refs. [66, 67], it was proposed to extend the study of these in-medium effects to nuclear collisions at NICA (Nuclotron-based Ion Collider Facility) and FAIR (Facility for Antiproton and Ion Research) energies. A suitable frame for such a study is the thermodynamic approach to light-nuclei production complemented by quantum statistical approach that includes medium effects due to Pauli blocking and self-energies [62, 68, 69]. This quantum statistical approach is based on the relativistic mean-field model of Ref. [68]. The energies of light nuclei are given by the formula

$$E_A(\mathbf{p}) = E_A^0(\mathbf{p}) + \Delta E_A^{\text{SE}}(\mathbf{p}) + \Delta E_A^{\text{Pauli}}(\mathbf{p}) \quad (1)$$

where $E_A^0(p)$ is the vacuum energy of A -nucleus with momentum \mathbf{p} , $\Delta E_A^{\text{SE}}(p)$ is in-medium self-energy shift, $\Delta E_A^{\text{Pauli}}(p)$ is the energy correction due to the Pauli blocking. The last two quantities also depend on the baryon density, temperature and proton/neutron asymmetry of the matter. More details can be found in Ref. [69]. This quantum statistical approach was incorporated into THESEUS at the particlization stage.

Preliminary results showed [70, 71] that the best description of the light-nuclei yields is obtained when the self-energy effects are discarded at few-GeV collision energies ($\sqrt{s_{NN}}$). However, those results were not conclusive because the proper conservation of the baryon charge was not achieved in that version of the THESEUS, see sect. II. The Pauli-blocking effects were disregarded in those calculations.

The present calculation are performed within the updated version of the THESEUS, where the conservation of the baryon charge is strictly fulfilled. An up-

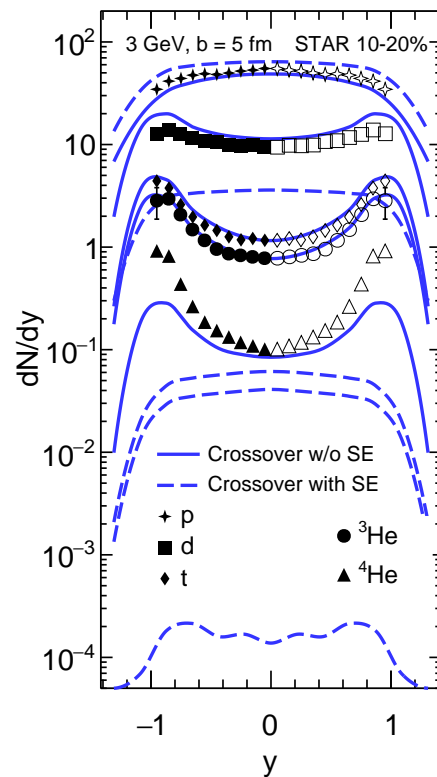


FIG. 3: Rapidity distributions of protons and light nuclei (top down: protons, deuterons, tritons, ${}^3\text{He}$ and ${}^4\text{He}$) in Au+Au collisions at collision energy of $\sqrt{s_{NN}} = 3$ GeV and $b = 5$ fm. Results are calculated in the crossover scenario with (with SE) and without (w/o SE) the self-energy contributions, i.e. the $\Delta E_A^{\text{SE}}(\mathbf{p})$ and $\Delta E_A^{\text{Pauli}}(\mathbf{p})$ terms in Eq. (1). Protons are calculated within the conventional 3FD freeze-out with the subsequent UrQMD afterburner. Deuterons, tritons, and ${}^3\text{He}$ are calculated with the late freeze-out ($\varepsilon_{\text{frz}} = 0.2$ GeV/fm 3), while ${}^4\text{He}$, the conventional 3FD freeze-out ($\varepsilon_{\text{frz}} = 0.4$ GeV/fm 3). STAR data are from Ref. [43]. Full symbols display measured experimental points, whereas the open ones are those reflected with respect to the midrapidity.

per estimate of the Pauli-blocking effect is also made by means of its approximation by that at zero light-nucleus momentum in the rest frame of the medium. The Pauli-blocking is strongest at this zero momentum. The Pauli-blocking effect turned out to be negligibly small because of high freeze-out temperatures as compared with the corresponding Fermi energies. The results of this calculation with the crossover EoS are displayed in Fig. 3. As seen, the medium effect accordingly to Ref. [69] turns out to be too strong. It results in strong disagreement with data, as has been already seen from the preliminary simulations [70, 71]. Even the proton yield is overestimated. Apparently this is because the relativistic mean-field model [68], underlying these medium corrections, has been parametrized to reproduce low-energy nuclear phenomena. This parametrization is simply inapplicable to highly excited nuclear matter. Of course, we could introduce a temperature-dependent attenuation factor to

reduce the strength of these medium corrections. However, it would be a purely phenomenological tuning parameter. Therefore, we avoid doing this.

IV. COLLECTIVE FLOW

Collective flow is a more subtle observable of the heavy-ion collisions. Its calculation with the thermodynamic approach is straightforward because light nuclei are treated on the equal basis with other hadrons. Results for the collective flow, which are presented below, are calculated with respect to the reaction plane that is exactly defined in the simulations. We have also done calculations with the event plane determined after the afterburner in terms of observable particles within the STAR acceptance. The reaction-plane and event-plane results turned out to be practically identical.

A. Directed flow

The calculated directed flow of protons and light nuclei (deuterons, ${}^3\text{He}$ and ${}^4\text{He}$) as function of rapidity in semi-central ($b = 6$ fm) Au+Au collisions at collision energy of $\sqrt{s_{NN}} = 3$ GeV is presented in Fig. 4. The results are compared with STAR data [44, 72]. We do not display results for the tritons because they are very similar to those for ${}^3\text{He}$, including the degree of agreement with the data. The THESEUS simulations for light nuclei are performed for the late freeze-out ($\varepsilon_{\text{frz}} = 0.2$ GeV/fm 3) for three EoS's. Protons are calculated within the conventional 3FD freeze-out with the subsequent UrQMD afterburner.

The directed flow turns out to be independent of the used EoS, which again suggests that the dynamics is dominated by the hadronic phase. The calculated results almost perfectly (except for very forward and backward rapidities) reproduce the experimental proton directed flow [72]. Agreement with the data [44] is getting worse with increase of atomic number of light nucleus. If the calculated midrapidity slope of the directed flow is only slightly steeper than the experimental one for deuterons, for ${}^4\text{He}$ it is already noticeably steeper.

To check if this disagreement is related to the above observed preference of the conventional freeze-out for the ${}^4\text{He}$, see Fig. 2, we present the results with conventional 3FD freeze-out in Fig. 5. As seen, the ${}^4\text{He}$ flow is independent of the type of the freeze-out while the flow slopes of lighter nuclei become only slightly steeper at the conventional freeze-out.

Stiffness of the hadronic EoS with the 3FD model can be easily changed. The stiffness is characterized by incompressibility of nuclear matter that is conventionally defined as

$$K = 9n_0^2 \frac{d^2}{dn^2} \left(\frac{\varepsilon(n, T=0)}{n} \right)_{n=n_0}, \quad (2)$$

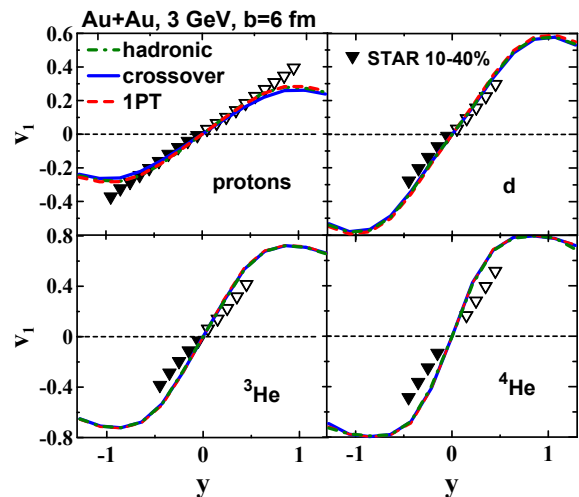


FIG. 4: Directed flow of protons and light nuclei (deuterons, ${}^3\text{He}$ and ${}^4\text{He}$) as function of rapidity in semicentral ($b = 6$ fm) Au+Au collisions at collision energy of $\sqrt{s_{NN}} = 3$ GeV. Results are calculated with hadronic, 1PT and crossover EoS's. Results of the THESEUS simulations with the late freeze-out ($\varepsilon_{\text{frz}} = 0.2$ GeV/fm 3) are displayed for light nuclei. Protons are calculated within the conventional 3FD freeze-out with the subsequent UrQMD afterburner. STAR data are from Ref. [44, 72]. Full symbols display measured experimental points, whereas the open ones are those reflected with respect to the midrapidity.

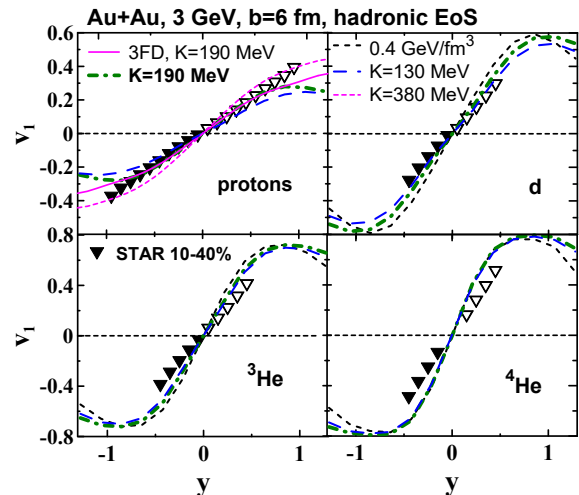


FIG. 5: The same as in Fig. 4 but for various versions of hadronic EoS: the standard hadronic EoS ($K = 190$ MeV) and very soft hadronic EoS ($K = 130$ MeV). Results of the THESEUS simulations with the late freeze-out ($\varepsilon_{\text{frz}} = 0.2$ GeV/fm 3) and conventional 3FD freeze-out ($\varepsilon_{\text{frz}} = 0.4$ GeV/fm 3) are displayed for light nuclei. Protons are calculated within the conventional 3FD freeze-out with the subsequent UrQMD afterburner. The proton v_1 within the 3FD model, i.e. before the UrQMD afterburner, is also presented for the standard EoS ($K = 190$ MeV, thin solid line) and stiff EoS ($K = 380$ MeV, thin short-dashed line).

where $\varepsilon(n, T = 0)$ is the energy density of the nuclear matter at zero temperature ($T = 0$) as a function of the baryon density (n), n_0 is the normal nuclear density. The conventionally used hadronic EoS is characterized by $K = 190$ MeV. This is a quite soft EoS. It is very similar (but not identical) to the EoS of the hadronic phase in the 1PT and crossover EoS's [57]. To study the effect of the EoS stiffness on the directed flow, we present results for a very soft hadronic EoS ($K = 130$ MeV) in Fig. 5. As seen, the ${}^4\text{He}$ flow again turns out to be independent of the EoS stiffness. The very soft EoS gives slightly better agreement with the data for lighter nuclei than the conventionally used EoS but results in disagreement with the experimental proton flow. In Ref. [72] it is reported that the stiff hadronic EoS ($K = 380$ MeV) well reproduces the proton directed flow within the UrQMD and JAM models. In contrast, our calculation shows that the stiff EoS ($K = 380$ MeV) results in too steep slope of the proton flow (see the thin short-dashed line in Fig. 5), which leads to even stronger disagreement with flow data for light nuclei. Therefore, the conventionally used soft hadronic EoS with $K = 190$ MeV seems to be the optimal choice. This conclusion agrees with that in famous paper [73] made more than twenty years ago.

The proton v_1 within the 3FD model, i.e. before the UrQMD afterburner, is also presented in Fig. 5. The afterburner does not change the midrapidity slope of the flow but worsens agreement with the data at very forward and backward rapidities. The proton flow at the late freeze-out and without afterburner (not displayed in Fig. 5) is very similar to that at the conventional 3FD freeze-out and the subsequent afterburner, which once again confirms the correctness of the choice of energy density for the late freeze-out.

In contrast to the proton flow, the afterburner imitation (i.e. the late freeze-out) does change the midrapidity slope of deuterons and ${}^3\text{He}$ albeit slightly. However, the ${}^4\text{He}$ flow is not affected by the late freeze-out.

B. Elliptic flow

The calculated elliptic flow of protons and light nuclei (deuterons, ${}^3\text{He}$ and ${}^4\text{He}$) as function of rapidity in semi-central ($b = 6$ fm) Au+Au collisions at collision energy of $\sqrt{s_{NN}} = 3$ GeV is presented in Fig. 6. The results are compared with STAR data [44, 72]. Results for tritons are again omitted because they are very similar to those for ${}^3\text{He}$. The THESEUS simulations for deuterons and ${}^3\text{He}$ are performed for the late freeze-out ($\varepsilon_{\text{frz}} = 0.2$ GeV/fm 3), while for ${}^4\text{He}$, the conventional 3FD freeze-out ($\varepsilon_{\text{frz}} = 0.4$ GeV/fm 3) in view of its preference for p_T spectra and y distributions, see sect. III. Protons are calculated within the conventional 3FD freeze-out with the subsequent UrQMD afterburner. For comparison, the light-nuclei flow with the conventional 3FD freeze-out for the 1PT EoS and the proton v_2 flow before the UrQMD afterburner are also demonstrated.

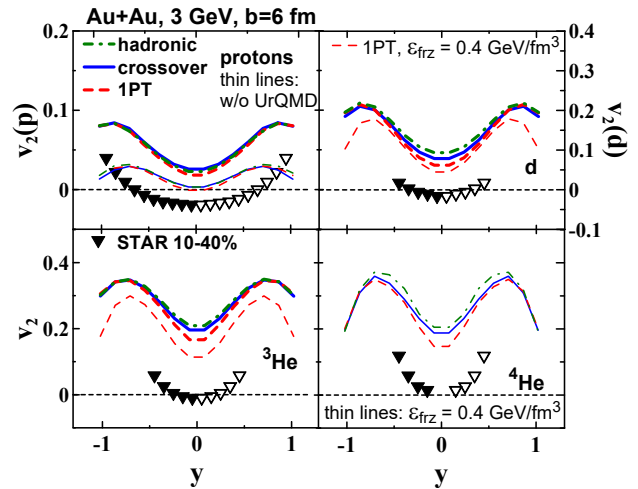


FIG. 6: Elliptic flow of protons and light nuclei (deuterons, ${}^3\text{He}$ and ${}^4\text{He}$) as function of rapidity in semi-central ($b = 6$ fm) Au+Au collisions at collision energy of $\sqrt{s_{NN}} = 3$ GeV. Results are calculated with hadronic, 1PT and crossover EoS's. Results of the THESEUS simulations with three EoS's are displayed for deuterons and ${}^3\text{He}$ at the late freeze-out ($\varepsilon_{\text{frz}} = 0.2$ GeV/fm 3) and for the ${}^4\text{He}$ nuclei at the conventional 3FD freeze-out ($\varepsilon_{\text{frz}} = 0.4$ GeV/fm 3). The conventional 3FD freeze-out with the 1PT EoS is also presented for deuterons and ${}^3\text{He}$. Protons are calculated within the conventional 3FD freeze-out with the subsequent UrQMD afterburner. The proton v_2 flows before the UrQMD afterburner are also presented. STAR data are from Refs. [44, 72]. Full symbols display measured experimental points, whereas the open ones are those reflected with respect to the midrapidity.

As seen from Fig. 6, the calculated elliptic flow considerably overestimates the data [44, 72]. Even the v_2 sign is different in the midrapidity region. The afterburner (for protons) and the late freeze-out (for light nuclei) even worsen agreement with the data. The large disagreement of light-nuclei elliptic flow with the data [44] does not mean that the thermodynamic approach fails to describe this flow. This only means that the 3FD model has troubles describing the elliptic flow of protons, which transform into even bigger troubles for light nuclei.

As stated in Refs. [44, 72, 73], a stiff EoS is needed for describing the elliptic flow. Therefore, we performed simulations with stiff hadronic EoS ($K = 380$ MeV), see Fig. 7. The results became closer to the data. The proton elliptic flow is even reproduced in the midrapidity. However, the overall disagreement with data remains. The afterburner (late freeze-out) still worsens the agreement with data.

Note that dips and even negative values of v_2 in the midrapidity are consequences of the squeeze-out effect [74–76], which result from blocking of the expanding central blob by the spectator matter. The squeeze-out is a characteristic feature of moderately relativistic collisions, in which the expanding central fireball is shadowed by spectators. This shadowing only partially is taken into

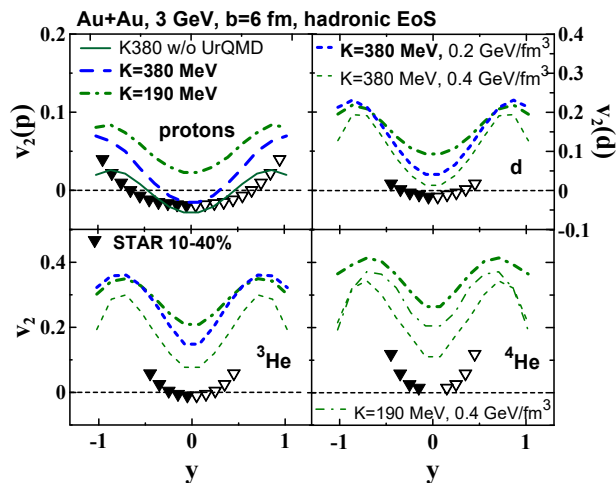


FIG. 7: The same as in Fig. 6 but for various versions of the hadronic EoS. Results with the standard hadronic EoS ($K = 190$ MeV) are displayed by bold dash-dotted lines for the late freeze-out ($\varepsilon_{\text{frz}} = 0.2$ GeV/fm³) for all light nuclei and by thin dash-dotted line for the standard 3FD freeze-out ($\varepsilon_{\text{frz}} = 0.4$ GeV/fm³) for ⁴He nuclei. Results of calculations with the stiff hadronic EoS ($K = 380$ MeV) are also presented: for deuterons and ³He at the late freeze-out and for all nuclei at the standard 3FD freeze-out. Protons are calculated within the conventional 3FD freeze-out with the subsequent UrQMD afterburner. The proton v_2 before the UrQMD afterburner is also presented for the stiff EoS ($K = 380$ MeV) by solid line.

account within the 3FD evolution because the frozen-out matter of the central fireball remains to be shadowed even after the freeze-out while in the 3FD model it escapes without interacting with spectators. The afterburning stage should, in principle, correct this deficiency. However, it does not, as we see from Figs. 7 and 6. The reason is that the THESEUS assigns the *same time instant* to all produced particles during the particlization procedure, while different parts of the system are frozen-out at *different time instants* in 3FD. Participants are frozen out earlier than spectators. If the particlization is isochronous, the evolution of the frozen-out participants stops until the spectators also become frozen-out. Therefore, we skip the stage of shading the afterburner expansion of the central fireball by spectators still being in the hydrodynamic phase. The afterburner evolution is switched on only when the spectators also become frozen out. The spectators are frozen out when they have already passed the expanding central fireball. Thus, the shadowing by spectators turns out to be strongly reduced after such isochronous particlization compared to what it would be if the entire collision process were kinetically treated, as in UrQMD or JAM. Apparently, this is the prime reason of failure of the elliptic-flow description. A time-extended transition from hydrodynamic evolution to afterburner dynamics would need to take into account the interaction of the kinetic afterburner phase with still hydrodynamically evolved matter. This is a difficult task

both technically and conceptually.

V. FEED-DOWN FROM UNSTABLE ⁴He

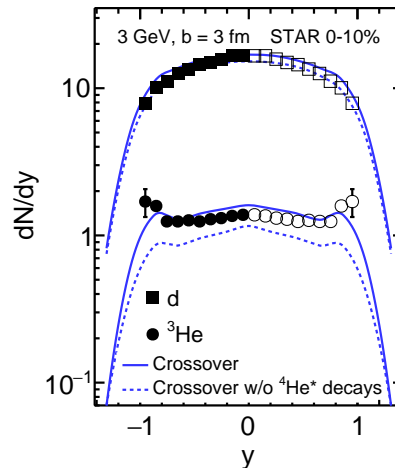


FIG. 8: Rapidity distributions of light nuclei (deuterons and ³He) in central Au+Au collisions at collision energy of $\sqrt{s_{NN}} = 3$ GeV. Results are calculated in the crossover scenario with and without (w/o ⁴He* decays) the feed-down contributions. STAR data are from Ref. [43]. Full symbols display measured experimental points, whereas the open ones are those reflected with respect to the midrapidity.

As found in Ref. [42], the feed-down contributions from unstable ⁴He to deuterons are negligibly small, while to tritons and ³He are less than 20% at $\sqrt{s_{NN}} > 6$ GeV in the midrapidity. At the forward/backward rapidities, these contributions are essential even at $\sqrt{s_{NN}} > 6$ GeV. It was predicted [38], that feed-down contributions reach values of the order of 60% for tritons and ³He even in midrapidity at $\sqrt{s_{NN}} = 3$ GeV.

Results of our calculations are presented in Fig. 8 at the example of the crossover EoS. In agreement with Ref. [38], the feed-down contribution amounts $\sim 20\%$ for deuterons and 50–100% (depending on the rapidity) for ³He. While the feed-down contribution into the deuteron yield is inessential for the data reproduction, it plays important role for ³He. Without this feed-down the ³He yield is noticeably underestimated.

The v_1 flow of deuterons, tritons and ³He turns out to be insensitive to the feed-down contributions from unstable ⁴He. Without these contributions, the corresponding v_2 flows are reduced by $\sim 20\%$, which, however, does not essentially change the degree of their agreement with the data. The effect on the proton yield and flow is negligible.

VI. SUMMARY

Simulations of the proton and light-nuclei production in Au+Au collisions at $\sqrt{s_{NN}} = 3$ GeV were performed

within the updated THESEUS event generator [41]. The results were compared with recent STAR data [43, 44]. The updated THESEUS treats the light-nuclei production within the thermodynamical approach on the equal basis with hadrons. The protons (as well as other hadron) are calculated with the standard 3FD freeze-out, characterized by the energy density of $\varepsilon_{\text{frz}} = 0.4 \text{ GeV}/\text{fm}^3$, followed by the UrQMD afterburner. The only additional parameter related to the light nuclei is the energy density of the late freeze-out that imitates the afterburner stage because the light nuclei do not participate in the UrQMD evolution.

In fact, the freeze-out parameter is required in both the thermodynamical and coalescence approaches. Both approaches are inapplicable at very early freeze-out, when inter-particle spacing in a fireball is less than the inter-nucleon distance in a light nucleus. At later freeze-out, the light-nuclei yields crucially depend on the freeze-out conditions in both approaches. The coalescence allows fine tuning of the light-nuclei production after the freeze-out by means of coalescence parameters. In contrast, within the thermodynamical approach, the light-nuclei observables are solely determined by the applied freeze-out in the absence of the afterburner. Dynamical treatment of the light nuclei at the afterburner stage [27, 28, 32, 33] would essentially weaken this strong dependence on the freeze-out.

It was found that the late freeze-out characterized by $\varepsilon_{\text{late frz}} = 0.2 \text{ GeV}/\text{fm}^3$ is preferable for deuterons, tritons, and ${}^3\text{He}$. This is precisely the same value of $\varepsilon_{\text{late frz}}$ that was found in Ref. [42] at higher collision energies. Remarkably, the ${}^4\text{He}$ yield and p_T spectra are better reproduced with the standard 3FD freeze-out. This suggests that the ${}^4\text{He}$ nuclei better survive in the afterburner stage because they are more spatially compact and tightly bound objects. This is an argument in favor of dynamical treatment of light nuclei.

Results of simulations with different EoS's (with and without transition to the quark-gluon phase) indicated that the dynamics is determined by the hadronic phase. The calculated results revealed not perfect, but a good reproduction of the data on bulk observables of the light nuclei. The calculated proton directed flow almost perfectly (except for very forward and backward rapidities) reproduces the experimental flow [72]. Agreement with the data on the directed flow [44] becomes worse with increase of atomic number of light nucleus. If the calculated midrapidity slope of the directed flow is only slightly steeper than the experimental one for deuterons, for ${}^4\text{He}$ it is already noticeably steeper.

The model failed to properly describe the data on the elliptic flow of both protons and light nuclei. We attribute this to shortcomings of the transition from the 3FD evolution to the UrQMD afterburner, which prevents us from proper description of the squeeze-out effect. The squeeze-out results from shadowing of the expanding central fireball by spectators. This shadowing only

partially taken into account within the 3FD evolution because the frozen-out matter of the central fireball remains to be shadowed even after the freeze-out while in the 3FD model it escapes without interacting with spectators. The afterburning stage should, in principle, correct this deficiency but it does not. The reason is that the THESEUS assigns the same time instant to all produced particles during the particlization procedure, while different parts of the system get frozen-out at different time instants in 3FD. The shadowing by spectators is strongly reduced after such isochronous particlization because the participants and spectators turn out to be well separated in thus constructed pre-afterburner configuration.

We also studied the feed-down contributions from unstable ${}^4\text{He}$ and possible in-medium effects. As found, the feed-down contribution amounts $\sim 20\%$ for deuterons and 50–100% (depending on the rapidity) for tritium and ${}^3\text{He}$. While the feed-down contribution into the deuteron yield is inessential for the data reproduction, it plays important role for tritium and ${}^3\text{He}$. Without this feed-down the tritium and ${}^3\text{He}$ yields are noticeably underestimated. The medium effect accordingly to Ref. [69] turned out to be too strong and resulted in strong disagreement with data. Apparently this is because the relativistic mean-field model [68], underlying these medium corrections, has been parametrized to reproduce low-energy nuclear phenomena. This parametrization is simply inapplicable to highly excited nuclear matter.

Development of new hybrid model called MUFFIN (MULTI Fluid simulation for Fast IoN collisions) was recently announced in Ref. [77]. This is a next-generation hybrid three-fluid model for simulating heavy-ion collisions at energies from few to few tens of GeV. Several methodical and conceptual improvements, as compared with THESEUS, are introduced in MUFFIN. An important conceptual improvement is the inclusion of initial state fluctuations, which are important when considering the collective flow and allow study of fluctuations associated with the CEP. The afterburner based on SMASH will make it possible to describe the afterburner evolution of at least deuterons. This could resolve some of the aforementioned problems in THESEUS.

Acknowledgments

We are sincerely grateful to Iurii Karpenko and David Blaschke who made enormous contributions early on in the implementation of this project. Fruitful discussions with D.N. Voskresensky are gratefully acknowledged. This work was carried out using computing resources of the federal collective usage center “Complex for simulation and data processing for mega-science facilities” at NRC “Kurchatov Institute” [78]. and computing resources of the supercomputer “Govorun” at JINR [79].

- [1] E. Shuryak and J. M. Torres-Rincon, Baryon preclustering at the freeze-out of heavy-ion collisions and light-nuclei production, *Phys. Rev. C* **101**, no.3, 034914 (2020) [arXiv:1910.08119 [nucl-th]].
- [2] E. Shuryak and J. M. Torres-Rincon, Light-nuclei production and search for the QCD critical point, *Eur. Phys. J. A* **56**, no.9, 241 (2020). [arXiv:2005.14216 [nucl-th]].
- [3] K. J. Sun, F. Li and C. M. Ko, Effects of QCD critical point on light nuclei production, *Phys. Lett. B* **816**, 136258 (2021). [arXiv:2008.02325 [nucl-th]].
- [4] M. A. Stephanov, K. Rajagopal and E. V. Shuryak, Signatures of the tricritical point in QCD, *Phys. Rev. Lett.* **81**, 4816-4819 (1998). [arXiv:hep-ph/9806219 [hep-ph]].
- [5] B. Berdnikov and K. Rajagopal, Slowing out-of-equilibrium near the QCD critical point, *Phys. Rev. D* **61**, 105017 (2000). [arXiv:hep-ph/9912274 [hep-ph]].
- [6] V. V. Skokov and D. N. Voskresensky, Hydrodynamical description of a hadron-quark first-order phase transition, *JETP Lett.* **90**, 223-227 (2009). [arXiv:0811.3868 [nucl-th]].
- [7] V. V. Skokov and D. N. Voskresensky, Hydrodynamical description of first-order phase transitions: Analytical treatment and numerical modeling, *Nucl. Phys. A* **828**, 401-438 (2009). [arXiv:0903.4335 [nucl-th]].
- [8] J. Randrup, Phase transition dynamics for baryon-dense matter, *Phys. Rev. C* **79**, 054911 (2009). [arXiv:0903.4736 [nucl-th]].
- [9] J. Steinheimer and J. Randrup, Spinodal amplification of density fluctuations in fluid-dynamical simulations of relativistic nuclear collisions, *Phys. Rev. Lett.* **109**, 212301 (2012). [arXiv:1209.2462 [nucl-th]].
- [10] J. Steinheimer, L. Pang, K. Zhou, V. Koch, J. Randrup and H. Stoecker, A machine learning study to identify spinodal clumping in high energy nuclear collisions, *JHEP* **12**, 122 (2019). [arXiv:1906.06562 [nucl-th]].
- [11] K. J. Sun, W. H. Zhou, L. W. Chen, C. M. Ko, F. Li, R. Wang and J. Xu, Spinodal Enhancement of Light Nuclei Yield Ratio in Relativistic Heavy Ion Collisions, arXiv:2205.11010 [nucl-th].
- [12] S. Mrowczynski, Production of light nuclei at colliders – coalescence vs. thermal model, *Eur. Phys. J. ST* **229**, no.22-23, 3559-3583 (2020). [arXiv:2004.07029 [nucl-th]].
- [13] A. Motornenko, J. Steinheimer, V. Vovchenko, R. Stock and H. Stoecker, Ambiguities in the hadro-chemical freeze-out of Au+Au collisions at SIS18 energies and how to resolve them, *Phys. Lett. B* **822**, 136703 (2021). [arXiv:2104.06036 [hep-ph]].
- [14] A. Kittiratpattana, T. Reichert, P. Li, A. Limphirat, C. Herold, J. Steinheimer and M. Bleicher, Investigating the cluster production mechanism with isospin triggering: Thermal models versus coalescence models, *Phys. Rev. C* **107**, no.4, 044911 (2023). [arXiv:2210.11699 [nucl-th]].
- [15] V. Kireyeu, G. Coci, S. Glaessel, J. Aichelin, C. Blume and E. Bratkovskaya, Cluster formation near midrapidity - can the mechanism be identified experimentally?, arXiv:2304.12019 [nucl-th].
- [16] J. Aichelin, 'Quantum' molecular dynamics: A Dynamical microscopic n body approach to investigate fragment formation and the nuclear equation of state in heavy ion collisions, *Phys. Rept.* **202**, 233-360 (1991).
- [17] V. N. Russkikh, Y. B. Ivanov, Y. E. Pokrovsky and P. A. Henning, Analysis of intermediate-energy heavy ion collisions within relativistic mean field two fluid model, *Nucl. Phys. A* **572**, 749-790 (1994).
- [18] Y. B. Ivanov, V. N. Russkikh and V. D. Toneev, Relativistic heavy-ion collisions within 3-fluid hydrodynamics: Hadronic scenario, *Phys. Rev. C* **73**, 044904 (2006).
- [19] H. Liu, D. Zhang, S. He, K. j. Sun, N. Yu and X. Luo, Light nuclei production in Au+Au collisions at $\sqrt{s_{NN}} = 5-200$ GeV from JAM model, *Phys. Lett. B* **805**, 135452 (2020). [arXiv:1909.09304 [nucl-th]].
- [20] L. Zhu, C. M. Ko and X. Yin, Light (anti-)nuclei production and flow in relativistic heavy-ion collisions, *Phys. Rev. C* **92**, no.6, 064911 (2015). [arXiv:1510.03568 [nucl-th]].
- [21] J. Steinheimer, K. Gudima, A. Botvina, I. Mishustin, M. Bleicher and H. Stoecker, Hypernuclei, dibaryon and antinuclei production in high energy heavy ion collisions: Thermal production versus Coalescence, *Phys. Lett. B* **714**, 85-91 (2012). [arXiv:1203.2547 [nucl-th]].
- [22] Z. J. Dong, G. Chen, Q. Y. Wang, Z. L. She, Y. L. Yan, F. X. Liu, D. M. Zhou and B. H. Sa, Energy dependence of light (anti)nuclei and (anti)hypertriton production in the Au-Au collision from $\sqrt{s_{NN}} = 11.5$ to 5020 GeV, *Eur. Phys. J. A* **54**, no.9, 144 (2018). [arXiv:1803.01547 [nucl-th]].
- [23] S. Sombun, K. Tomuang, A. Limphirat, P. Hillmann, C. Herold, J. Steinheimer, Y. Yan and M. Bleicher, Deuteron production from phase-space coalescence in the UrQMD approach, *Phys. Rev. C* **99**, no.1, 014901 (2019). [arXiv:1805.11509 [nucl-th]].
- [24] P. Hillmann, K. Käfer, J. Steinheimer, V. Vovchenko and M. Bleicher, Coalescence, the thermal model and multi-fragmentation: the energy and volume dependence of light nuclei production in heavy ion collisions, *J. Phys. G* **49**, no.5, 055107 (2022). [arXiv:2109.05972 [hep-ph]].
- [25] W. Zhao, C. Shen, C. M. Ko, Q. Liu and H. Song, Beam-energy dependence of the production of light nuclei in Au + Au collisions, *Phys. Rev. C* **102**, no.4, 044912 (2020). [arXiv:2009.06959 [nucl-th]].
- [26] W. Zhao, K. j. Sun, C. M. Ko and X. Luo, Multiplicity scaling of light nuclei production in relativistic heavy-ion collisions, *Phys. Lett. B* **820**, 136571 (2021). [arXiv:2105.14204 [nucl-th]]. [arXiv:1606.06642 [nucl-th]].
- [27] D. Oliinychenko, L. G. Pang, H. Elfner and V. Koch, Microscopic study of deuteron production in PbPb collisions at $\sqrt{s} = 2.76$ TeV via hydrodynamics and a hadronic afterburner, *Phys. Rev. C* **99**, no.4, 044907 (2019). [arXiv:1809.03071 [hep-ph]].
- [28] J. Staudenmaier, D. Oliinychenko, J. M. Torres-Rincon and H. Elfner, Deuteron production in relativistic heavy ion collisions via stochastic multiparticle reactions, *Phys. Rev. C* **104**, no.3, 034908 (2021). [arXiv:2106.14287 [hep-ph]].
- [29] J. Aichelin, E. Bratkovskaya, A. Le Fèvre, V. Kireyeu, V. Kolesnikov, Y. Leifels, V. Voronyuk and G. Coci, Parton-hadron-quantum-molecular dynamics: A novel microscopic n-body transport approach for heavy-ion collisions, dynamical cluster formation, and hypernuclei production, *Phys. Rev. C* **101**, no.4, 044905 (2020). [arXiv:1907.03860 [nucl-th]].

- [30] S. Gläsel, V. Kireyeu, V. Voronyuk, J. Aichelin, C. Blume, E. Bratkovskaya, G. Coci, V. Kolesnikov and M. Winn, Cluster and hypercluster production in relativistic heavy-ion collisions within the parton-hadron-quantum-molecular-dynamics approach, *Phys. Rev. C* **105**, no.1, 014908 (2022). [arXiv:2106.14839 [nucl-th]].
- [31] E. Bratkovskaya, S. Gläsel, V. Kireyeu, J. Aichelin, M. Bleicher, C. Blume, G. Coci, V. Kolesnikov, J. Steinheimer and V. Voronyuk, Midrapidity cluster formation in heavy-ion collisions, *EPJ Web Conf.* **276**, 03005 (2023). [arXiv:2208.11802 [nucl-th]].
- [32] K. J. Sun, R. Wang, C. M. Ko, Y. G. Ma and C. Shen, Relativistic kinetic approach to light nuclei production in high-energy nuclear collisions, arXiv:2106.12742 [nucl-th].
- [33] K. J. Sun, R. Wang, C. M. Ko, Y. G. Ma and C. Shen, Unveiling the dynamics of nucleosynthesis in relativistic heavy-ion collisions, arXiv:2207.12532 [nucl-th].
- [34] R. Wang, Y. G. Ma, L. W. Chen, C. M. Ko, K. J. Sun and Z. Zhang, Kinetic approach of light-nuclei production in intermediate-energy heavy-ion collisions, *Phys. Rev. C* **108**, no.3, L031601 (2023). [arXiv:2305.02988 [nucl-th]].
- [35] J. Adam *et al.* [STAR], Beam energy dependence of (anti-)deuteron production in Au + Au collisions at the BNL Relativistic Heavy Ion Collider, *Phys. Rev. C* **99**, no.6, 064905 (2019). [arXiv:1903.11778 [nucl-ex]].
- [36] [STAR], Beam Energy Dependence of Triton Production and Yield Ratio ($N_t \times N_p/N_d^2$) in Au+Au Collisions at RHIC, *Phys. Rev. Lett.* **130**, 202301 (2023). [arXiv:2209.08058 [nucl-ex]].
- [37] A. Andronic, P. Braun-Munzinger, J. Stachel and H. Stocker, Production of light nuclei, hypernuclei and their antiparticles in relativistic nuclear collisions, *Phys. Lett. B* **697**, 203-207 (2011). [arXiv:1010.2995 [nucl-th]].
- [38] V. Vovchenko, B. Dönigus, B. Kardan, M. Lorenz and H. Stoecker, Feeddown contributions from unstable nuclei in relativistic heavy-ion collisions, *Phys. Lett. B*, 135746 (2020). [arXiv:2004.04411 [nucl-th]].
- [39] D. Zhang [STAR], Light Nuclei (d, t) Production in Au + Au Collisions at $\sqrt{s_{NN}} = 7.7\text{-}200\text{GeV}$, *Nucl. Phys. A* **1005**, 121825 (2021). [arXiv:2002.10677 [nucl-ex]]; Energy Dependence of Light Nuclei (d, t) Production at STAR, *JPS Conf. Proc.* **32**, 010069 (2020). [arXiv:1909.07028 [nucl-ex]].
- [40] A. Andronic, P. Braun-Munzinger, K. Redlich and J. Stachel, Decoding the phase structure of QCD via particle production at high energy, *Nature* **561**, no.7723, 321-330 (2018). [arXiv:1710.09425 [nucl-th]].
- [41] M. Kozhevnikova, Y. B. Ivanov, I. Karpenko, D. Blaschke and O. Rogachevsky, Update of the Three-fluid Hydrodynamics-based Event Simulator: light-nuclei production in heavy-ion collisions, *Phys. Rev. C* **103**, no.4, 044905 (2021). [arXiv:2012.11438 [nucl-th]].
- [42] M. Kozhevnikova and Y. B. Ivanov, Light-nuclei production in heavy-ion collisions within a thermodynamical approach, *Phys. Rev. C* **107**, no.2, 024903 (2023). [arXiv:2210.07334 [nucl-th]]; *Particles* **6**, no.1, 440-450 (2023).
- [43] [STAR], "Production of Protons and Light Nuclei in Au+Au Collisions at $\sqrt{s_{NN}} = 3\text{ GeV}$ with the STAR Detector," arXiv:2311.11020 [nucl-ex]. [arXiv:2110.10929 [nucl-ex]]. [arXiv:2208.04650 [nucl-ex]].
- [44] M. S. Abdallah *et al.* [STAR], Light nuclei collectivity from $\sqrt{s_{NN}} = 3\text{ GeV}$ Au+Au collisions at RHIC, *Phys. Lett. B* **827**, 136941 (2022). [arXiv:2112.04066 [nucl-ex]].
- [45] Y. Nara, N. Otuka, A. Ohnishi, K. Niita and S. Chiba, Study of relativistic nuclear collisions at AGS energies from p + Be to Au + Au with hadronic cascade model, *Phys. Rev. C* **61**, 024901 (2000). [arXiv:nucl-th/9904059 [nucl-th]].
- [46] M. Isse, A. Ohnishi, N. Otuka, P. K. Sahu and Y. Nara, Mean-field effects on collective flows in high-energy heavy-ion collisions from AGS to SPS energies, *Phys. Rev. C* **72**, 064908 (2005). [arXiv:nucl-th/0502058 [nucl-th]].
- [47] J. Weil *et al.* [SMASH], Particle production and equilibrium properties within a new hadron transport approach for heavy-ion collisions, *Phys. Rev. C* **94**, no.5, 054905 (2016). [arXiv:1606.06642 [nucl-th]].
- [48] S. A. Bass, M. Belkacem, M. Bleicher, M. Brandstetter, L. Bravina, C. Ernst, L. Gerland, M. Hofmann, S. Hofmann and J. Konopka, *et al.*, Microscopic models for ultrarelativistic heavy ion collisions, *Prog. Part. Nucl. Phys.* **41**, 255-369 (1998). [arXiv:nucl-th/9803035 [nucl-th]].
- [49] Y. Xu, X. He and N. Xu, Light nuclei production in Au+Au collisions at 3 GeV from coalescence model*, *Chin. Phys. C* **47**, no.7, 074107 (2023). [arXiv:2305.02487 [nucl-th]].
- [50] N. Buyukcizmeci, T. Reichert, A. S. Botvina and M. Bleicher, Nucleosynthesis of light nuclei and hypernuclei in central Au+Au collisions at $\sqrt{s_{NN}}=3\text{ GeV}$, *Phys. Rev. C* **108**, no.5, 054904 (2023). [arXiv:2306.17145 [nucl-th]].
- [51] P. Batyuk *et al.*, Event simulation based on three-fluid hydrodynamics for collisions at energies available at the Dubna Nuclotron-based Ion Collider Facility and at the Facility for Antiproton and Ion Research in Darmstadt, *Phys. Rev. C* **94**, 044917 (2016). [arXiv:1608.00965 [nucl-th]].
- [52] P. Batyuk, D. Blaschke, M. Bleicher, Y. B. Ivanov, I. Karpenko, L. Malinina, S. Merts, M. Nahrgang, H. Petersen and O. Rogachevsky, Three-fluid Hydrodynamics-based Event Simulator Extended by UrQMD final State interactions (THESEUS) for FAIR-NICA-SPSBES/RHIC energies, *EPJ Web Conf.* **182**, 02056 (2018). [arXiv:1711.07959 [nucl-th]].
- [53] Y. B. Ivanov, Alternative Scenarios of Relativistic Heavy-Ion Collisions: I. Baryon Stopping, *Phys. Rev. C* **87**, no.6, 064904 (2013). [arXiv:1302.5766 [nucl-th]].
- [54] Y. B. Ivanov and A. A. Soldatov, Light fragment production at CERN Super Proton Synchrotron, *Eur. Phys. J. A* **53**, no. 11, 218 (2017). [arXiv:1703.05040 [nucl-th]].
- [55] <https://www.nndc.bnl.gov/nudat2/getdataset.jsp?nucleus=4HE&unc=nds>
- [56] I. N. Mishustin, V. N. Russkikh and L. M. Satarov, Fluid dynamical model of relativistic heavy ion collision, *Sov. J. Nucl. Phys.* **54**, 260-314 (1991).
- [57] A. S. Khvorostukin, V. V. Skokov, V. D. Toneev and K. Redlich, Lattice QCD constraints on the nuclear equation of state, *Eur. Phys. J. C* **48**, 531 (2006).
- [58] V. N. Russkikh and Yu. B. Ivanov, Dynamical freeze-out in 3-fluid hydrodynamics, *Phys. Rev. C* **76**, 054907 (2007).
- [59] Yu. B. Ivanov and V. N. Russkikh, On freeze-out problem in relativistic hydrodynamics, *Phys. Atom. Nucl.* **72**, 1238 (2009). [arXiv:0810.2262 [nucl-th]].
- [60] Y. B. Ivanov and A. A. Soldatov, Correlation between global polarization, angular momentum, and flow in

- heavy-ion collisions, *Phys. Rev. C* **102**, no.2, 024916 (2020). [arXiv:2004.05166 [nucl-th]].
- [61] W. Reisdorf *et al.* [FOPI], Systematics of central heavy ion collisions in the 1A GeV regime, *Nucl. Phys. A* **848**, 366-427 (2010). [arXiv:1005.3418 [nucl-ex]].
- [62] S. Typel, G. Ropke, T. Klahn, D. Blaschke and H. H. Wolter, Composition and thermodynamics of nuclear matter with light clusters, *Phys. Rev. C* **81**, 015803 (2010). [arXiv:0908.2344 [nucl-th]].
- [63] P. Danielewicz and Q. b. Pan, Blast of light fragments from central heavy-ion collisions, *Phys. Rev. C* **46**, 2002-2011 (1992)
- [64] C. Kuhrtz, M. Beyer, P. Danielewicz and G. Ropke, Medium corrections in the formation of light charged particles in heavy ion reactions, *Phys. Rev. C* **63**, 034605 (2001). [arXiv:nucl-th/0009037 [nucl-th]].
- [65] A. Ono, Cluster production within antisymmetrized molecular dynamics, *EPJ Web Conf.* **122**, 11001 (2016).
- [66] N. U. Bastian, P. Batyuk, D. Blaschke, P. Danielewicz, Y. B. Ivanov, I. Karpenko, G. Röpke, O. Rogachevsky and H. H. Wolter, Light cluster production at NICA, *Eur. Phys. J. A* **52**, no.8, 244 (2016). [arXiv:1608.02851 [nucl-th]].
- [67] G. Röpke, D. Blaschke, Y. B. Ivanov, I. Karpenko, O. V. Rogachevsky and H. H. Wolter, Medium effects on freeze-out of light clusters at NICA energies, *Phys. Part. Nucl. Lett.* **15**, no.3, 225-229 (2018). [arXiv:1712.07645 [nucl-th]].
- [68] G. Röpke, N. U. Bastian, D. Blaschke, T. Klahn, S. Typel and H. H. Wolter, Cluster virial expansion for nuclear matter within a quasiparticle statistical approach, *Nucl. Phys. A* **897**, 70-92 (2013). [arXiv:1209.0212 [nucl-th]].
- [69] G. Röpke, Nuclear matter equation of state including two-, three-, and four-nucleon correlations, *Phys. Rev. C* **92**, no.5, 054001 (2015). [arXiv:1411.4593 [nucl-th]].
- [70] D. Blaschke, G. Röpke, Y. Ivanov, M. Kozhevnikova and S. Liebing, Strangeness and light fragment production at high baryon density, *Springer Proc. Phys.* **250**, 183-190 (2020). [arXiv:2001.02156 [nucl-th]].
- [71] D. Blaschke, A. V. Friesen, Y. B. Ivanov, Y. L. Kalinovsky, M. Kozhevnikova, S. Liebing, A. Radzhabov and G. Röpke, QCD Phase Diagram at NICA Energies: K^+/π^+ Horn Effect and Light Clusters in THE-SEUS, *Acta Phys. Polon. Supp.* **14**, no.3, 485-489 (2021). [arXiv:2004.01159 [hep-ph]].
- [72] M. S. Abdallah *et al.* [STAR], Disappearance of partonic collectivity in sNN=3GeV Au+Au collisions at RHIC, *Phys. Lett. B* **827**, 137003 (2022). [arXiv:2108.00908 [nucl-ex]].
- [73] P. Danielewicz, R. Lacey and W. G. Lynch, Determination of the equation of state of dense matter, *Science* **298**, 1592-1596 (2002). [arXiv:nucl-th/0208016 [nucl-th]].
- [74] H. Sorge, Elliptical flow: A Signature for early pressure in ultrarelativistic nucleus-nucleus collisions, *Phys. Rev. Lett.* **78**, 2309-2312 (1997). [arXiv:nucl-th/9610026 [nucl-th]].
- [75] P. Danielewicz, R. A. Lacey, P. B. Gossiaux, C. Pinkenburg, P. Chung, J. M. Alexander and R. L. McGrath, Disappearance of elliptic flow: a new probe for the nuclear equation of state, *Phys. Rev. Lett.* **81**, 2438-2441 (1998). [arXiv:nucl-th/9803047 [nucl-th]].
- [76] Y. B. Ivanov and A. A. Soldatov, Elliptic Flow in Heavy-Ion Collisions at Energies $\sqrt{s_{NN}} = 2.7-39$ GeV, *Phys. Rev. C* **91**, no.2, 024914 (2015). [arXiv:1401.2265 [nucl-th]].
- [77] J. Cimerman, I. Karpenko, B. Tomasik and P. Huovinen, Next-generation multifluid hydrodynamic model for nuclear collisions at sNN from a few GeV to a hundred GeV, *Phys. Rev. C* **107**, no.4, 044902 (2023). [arXiv:2301.11894 [nucl-th]].
- [78] <http://ckp.nrcki.ru/>
- [79] http://hlit.jinr.ru/supercomputer_govorun/